Desalination and Water Treatment
www.deswater.com

doi:10.5004/dwt.2019.24185

159 (2019) 377–389
August

The Cd(II) adsorption capacities of activated carbons optimized by RSM: preparation and adsorption optimization

Wenjun Yin[a,c], Congcong Zhao[b,*], Jingtao Xu[a,*], Jian Zhang[c]

[a]*School of Municipal and Environmental Engineering, Shandong Jianzhu University, Jinan, 250101, China, email: xujingtao@sdjzu.edu.cn (J. Xu)*
[b]*College of Geography and Environment, Collaborative Innovation Center of Human-Nature and Green Development in Universities of Shandong, Shandong Normal University, Jinan 250014, China, email: zhaocongcong1009@163.com (C. Zhao)*
[c]*Shandong Key Laboratory of Water Pollution Control and Resource Reuse, School of Environmental Science and Engineering, Shandong University, Jinan 250100, China*

Received 25 November 2018; Accepted 27 March 2019

ABSTRACT

Activated carbon was synthesized from *Phragmites australis* with phosphoric acid activation and was used to remove Cd(II) from aquatic media. The effects of change in preparation conditions (impregnation rate, activation temperature, activation time) and adsorption conditions(pH, adsorption temperature, initial concentration and carbon dosage) on the adsorption capacity of Cd(II) were investigated and optimized by response surface methodology (RSM) based on Box-Behnken experimental design (BBD). The optimum preparation conditions for the impregnation ratio, activation time, and activation temperature were 2.3, 100 min, and 510°C, respectively, and the optimum adsorption capacity was 42.85 mg/g. The optimum adsorption conditions for pH, carbon dosage, adsorption temperature, and initial concentration were 3.5, 0.05 g, 45°C, and 53 mg/L, respectively, and the optimum adsorption capacity was 43.55 mg/g. The adsorption experiments and XPS survey spectra reveal that the Cd(II) adsorption mechanisms, microporous entrapment, cation exchange, electrostatic attraction, and surface complexation play key roles in Cd(II) removal.

Keywords: Activated carbon (ACs); *Phragmites australis* (PA); Response surface methodology (RSM); Cd(II); Optimization

1. Introduction

Trace amounts of cadmium (Cd(II)) can be accumulated in food chain and eventually,can become a potential toxic threat for inhuman beings and environment, so Cd(II) had been classified as carcinogen according to the US National Toxicology Program [1–3]. It is necessary to develop efficient methods to remove Cd(II) from aquatic media to prevent it from entering the food chain. Cd(II) could be removed from wastewater by chemical precipitation, electrolysis, ion exchange, membrane and adsorption [4,5]. However, activated carbons are one of the more efficient, economically favorable (low infrastructure costs) and technically easy adsorbents, and they have potential adsorption capabilities in a wide range of fields, including metal ions, and antibiotics [6–8].

The atomic weight, ionic radius, and hydrated ionic radius of Cd(II) are 112.41 g/mol, 0.097 nm, and 0.426 nm [9]. ACs with developed microporous structures and functional groups can effectively remove Cd(II), and the performance of ACs is related to their preparation conditions. The preparation conditions for ACs, which could affect the physiochemical properties, include the following: (1) impregnation rate, (2) activation temperature, and (3) activation time [10,11]. For example, ACs prepared with at lower impregnation ratios, activation temperatures, and

*Corresponding author.

activation times have lower porosity and specific surface area, due to insufficient activation and decomposition reactions between the activator and the carbon precursor. However, ACs prepared with higher impregnation ratios, activation temperatures, and activation times have either larger the pore sizes or no adsorption capacities, due to excessive activation and decomposition reactions between the activator and the carbon precursor. Thus, suitable preparation conditions could improve the physicochemical properties of the ACs for Cd(II) removal. Adsorption conditions, such as pH, adsorption temperature, initial concentration and carbon dosage, can also play important roles in the removal of Cd(II). For example, the adsorption capacity of ACs for heavy metal ions was extremely low under the extreme conditions of high pH, and adsorption temperature [12]. Therefore, suitable adsorption conditions could greatly increase the adsorption capacity.

Phragmites australis (PA), is a common wetlands grass plant. PA is suitable as a material for activated carbon preparation [13]. Phosphoric acid, H_3PO_4, is an important activating agent for the preparation of porous carbons from lignocellulose substances [14].

Response surface methodology (RSM) based on Box-Behnken experimental design (BBD) can effectively optimize the conditions for preparation and adsorption. RSM has the advantages of shorter test times, periods, high precision of the regression equations, and prediction performance, additionally, it can also study the interaction of multiple factors [15,16]. To the best of our knowledge, there is no report on optimization preparation and adsorption conditions simultaneously by RSMs to date.

The aims of this study were to: (1) prepare activated carbon with phosphoric acid by using RSM; (2) optimize the adsorption conditions by using RSM; (3) explore the physicochemical properties of biochar through N_2 adsorption/desorption, Fourier transform infrared (FTIR), X-ray photoelectron spectroscopy (XPS), X-ray diffraction (XRD), Boehm titration and elemental analysis; and (4) evaluate the adsorption capacities and explain the adsorption mechanism of Cd(II) on ACs.

2. Materials and methods

2.1. Materials

The precursor of the ACs was *Phragmites australis* (PA) obtained from Mata Lake Wetland (Shandong, China). The PA was thoroughly washed with tap water and dried overnight at 105°C for 24 h, and then cut into pieces of approximately 0.45–1.0 mm (the pieces that can be put into the crusher are considered qualified). The Cd(II) stock solution (100 mg/L) was prepared by dissolving 0.2829 g of $CdCl_2$ in 1 L of deionized water, and then appropriately diluting to the obtain desired concentration for each experiment. All chemical reagents were of analytical grade in this study and purchased from Sigma-Aldrich Co. Ltd.

2.2. Preparation method

According to design of the response surface methodology (RSM) [17,18]: (1) the impregnation ratio (level: 1, 2, and 3); (2) the activation temperature (level: 400°C, 500°C, and 600°C); and (3) the activation time (level: 60 min, 90 min, and 120 min) were selected as the factor values, and the adsorption capacity of Cd(II) (Q_e) was used as the response value. The mixed samples were obtained by mixing the PA with phosphoric acid (85 wt.% PPA) at the specific impregnation ratio (g PPA/g precursors) for the preparation of the ACs. After the samples were stored at room temperature for 11 h, and then transferred to a muffle furnace (under N_2) for the carbonization of the activated carbon under the specific conditions chosen for activation temperature and time. Then the cooled samples were washed several times with hot deionized water until their pH values (approximately 7) were steady. Finally, the samples were dried at 105°C for 12h and sifted to 160–200 mesh using standard sieves (Model Φ200, China). The sample particles obtained by this method were used as the ACs.

2.3. Characterization methods

In this study, the surface morphology was analyzed by Scanning electron microscopy (SEM, JEOL, JSM-6700F, Japan). The Brunauer-Emmett-Teller (BET) and pore structure of ACs were determined by N_2 adsorption/desorption at 77 K using surface area analyzer (Quantachrome Corporation, USA). Micropore volume (V_{mic}), micropore surface area (S_{mic}), total pore volume (V_{tot}) and average pore diameter (D_p) were calculated by the method in literatures in the Supplementary materials [19,20]. Elemental analyses (C, H, O and N) were measured by using Vario EI III Element Analyzer (USA). Boehm titration method was used to differentiate and quantify the acidic and basic functional groups on the activated carbon' surface [21]. The point of zero charge (pH_{PZC}) value of the adsorbent will provide a better understanding of the effect of pH on adsorption in the Supplementary materials. The surface functional groups of the activated carbon were also investigated by Fourier transform infrared spectroscopy (FTIR, Fourier-380FTIR, USA) and X-ray photoelectron spectroscopy XPS (Nico-let-460, Thermo Fisher, USA) in the Supplementary materials.

2.4. Adsorption experiments

Adsorption experiments used the Box-Behnken design (BBD). The (1) pH (level: 2, 4, and 6); (2) adsorption temperature (level: 20, 30, and 40°C); (3) initial concentration (level: 30, 45, and 60 mg/L); and (4) adsorbent dose (level: 0.02, 0.04, and 0.06 mg) were used as the factor values, and the adsorption capacity of Cd(II) (Q_e) was selected as the response value.

Adsorption kinetic experiments were conducted by adding 1.2 g of the biochar sample to a 2 L Cd(II) solution (C_0 = 30 mg/L, pH = 6.01), and then sampling at scheduled time until the adsorption equilibrium was reached. Adsorption isotherm experiments were conducted solution with initial Cd(II) concentrations varied from 10 to 70 mg/L. The pH impact experiments on Cd(II) adsorption were evaluated under the pH range of 2.0–7.0 with an initial Cd(II) concentration of 30 mg/L. The initial pH was adjusted, with the addition of 0.01 M HCl and NaOH to the desired pH values.

The mixtures of adsorbent and solution were shaken in air bath shaker (THZ-82) for 48 h under the specific pH, adsorption temperature, initial concentration and adsor-

bent dose conditions. Each mixture was filtered through a membrane filter (0.45 μm) after reaching the adsorption equilibrium, and the residual Cd(II) concentration was measured using an ICP-OES analyzer (iCAP6300, Thermo, USA). The Q_e (mg/g) was calculated by Eq. (1):

$$Q_e = \frac{(C_0 - C_e) \times V}{M} \quad (1)$$

where C_0 and C_e is the initial and equilibrium concentrations of Cd(II) (mg/L); V is the solution volume (L); and M is the mass of the adsorbent dose (g).

Three-sample t-tests were used to evaluate the significate difference of each group. The data are the averages of two or more replicates. The result was considered statistically significant when $p < 0.05$ (a level of significance above 95%).

3. Results and discussion

3.1. Optimization of preparation conditions

As shown in Table 1, 17 sets of experimental points were chosen by using the three factors and the three levels based on BBD, and 5 sets of the same experimental points (0, 0, 0) were chosen to better estimate the experimental error. The experimental data were fit using multiple regression fitting, and then the response surface regression model I (actual uncoded fitting equation) was acquired, as shown in Table S1 [22]. As shown in Table S2, the interaction effects between the factors and response values together with the model's statistical analysis were studied by analysis of variance (ANOVA) [23]. The P values for each factor were less than 0.01, indicating that the impregnation ratio, activation temperature and activation time had significant influence on the response value. The relationship between the actual and predicted adsorption capacities is shown in Fig. S1-a.The graph shows that there are tends in the linear regression fit, and the model adequately explained the experimental range studied. The corresponding F value of Model-I was 197.54, with $P < 0.001$ indicating that Model-I had a higher confidence level, which could effectively predict the Cd(II) adsorption process. The R^2 and Adj R^2 of Model-I were 0.9961 and 0.991, respectively, with Adj R^2-Pred $R^2 < 0.2$, indicating that the degree of fit the model was high. The Adeq-Precision of Model-I was 39.54, which was greater than 4, meaning that the reliability of Eq. (1) was very high. Thus, the model could better predict the adsorption capacity of Cd(II) [24–26].

Table 1
Response surface analysis program and test results

Number	Factors and levels			Response values Q (mg/g)
	Impregnation ratio	Activation temperature	Activation time	
AC-1	2	400	120	31.25
AC-2	1	500	60	10.37
AC-3	1	600	90	22.59
AC-4	3	400	90	30.39
AC-5	3	500	120	33.73
AC-6	1	400	90	6.50
AC-7	2	500	90	39.29
AC-8	2	600	60	26.53
AC-9	2	600	120	32.51
AC-10	2	500	90	41.60
AC-11	3	600	90	26.45
AC-12	2	500	90	39.84
AC-13	3	500	60	9.98
AC-14	1	500	90	20.42
AC-15	2	400	60	16.73
AC-16	2	500	90	41.24
AC-17	2	500	90	42.24

The preparation conditions of AC-I, AC-II, and AC-III were obtained using the regression equation and the practical application of Design-Expert 8.0.6 software, as shown in Table 2. The calculated Q_es for AC-I, AC-II, and AC-III are the optimal value, the suboptimal value, and the intermediate value, respectively. The actual average adsorption capacities of AC-I, AC-II and AC-III were 42.65, 41.45 and 31.02 mg/g, respectively. The preparation conditions of the optimum activated carbon were a 2.3 of impregnation ratio, 100 min of activation time, and 510°C of activation temperature.

3.2. Optimization of adsorption conditions

By comparing the optimal adsorption conditions of the three kinds of carbon, the preparation conditions for the optimal carbon are again determined. As shown in Table 3, the study used 87 total sets of batch experiments for AC-I (29 sets), AC-II (29 sets), and AC-III (29 sets). The equations for Model-II (for AC-I), Model-III (for AC-II), and Model-IV (for AC-III) are shown in Table S1. The response surface parameters of the three models are shown in Table S3. The values of P (adsorption factors), F (Models), P (Models), R^2 (Equations), Adj R^2 (Equations), the coefficient of variation (CV%, Equations) [27], and Adeq-Precision (Equations) and Fig. S1b, S1c and S1d indicate that the experimental results and the models were reliable. The actual optimal adsorption conditions of the ACs were X (for AC-I), Y (for AC-I), and Z (for AC-I), as shown in Table 4. The preparation conditions for optimum activated carbon were of impregnation ratio, 100 min of activation time, 510°C of activation temperature. The optimal adsorption conditions were a 44°C of temperature, 0.05 g of dose, 3.5 of pH, and 53 mg/L of C_0.

Table 2
The preparation conditions for the ACs

Preparation conditions	Impregnation ratio	Activation time (min)	Activation temperature (°C)	Q (mg/g)
AC-I	2.30	100	510	42.85
AC-II	2.30	109	537	41.44
AC-III	2.00	120	400	31.02

Table 3
Response surface analysis program and test results

Number	Factors and levels				Response values Q_1 (mg/g)	Response values Q_2 (mg/g)	Response values Q_3 (mg/g)
	Adsorption temperature	Adsorbent dose	pH	Initial concentration			
1	30	0.02	6	45	29.11	28.58	16.17
2	30	0.02	4	30	27.47	27.23	20.18
3	20	0.04	6	45	26.53	25.97	19.49
4	20	0.04	2	45	32.27	31.66	24.29
5	40	0.02	4	45	37.05	36.42	27.21
6	40	0.04	6	45	32.50	31.72	23.06
7	30	0.04	2	30	25.53	26.05	18.75
8	40	0.06	4	45	40.37	39.53	29.65
9	30	0.04	2	60	38.93	39.24	28.59
10	40	0.04	4	30	30.65	30.02	22.51
11	20	0.06	4	45	36.07	34.24	26.79
12	30	0.04	6	30	22.62	22.49	16.62
13	30	0.02	2	45	30.91	30.55	22.71
14	30	0.04	4	45	45.91	45.37	33.72
15	30	0.06	2	45	38.76	38.31	26.46
16	20	0.04	4	60	34.50	34.33	25.34
17	30	0.04	4	45	45.53	45.15	33.44
18	30	0.06	4	30	28.30	27.84	20.79
19	30	0.02	4	60	35.53	35.62	26.10
20	30	0.06	6	45	28.08	27.96	20.62
21	20	0.04	4	30	26.23	26.25	19.26
22	40	0.04	4	60	43.24	43.63	32.27
23	30	0.04	4	45	45.96	45.67	33.76
24	30	0.04	4	45	45.05	44.66	33.09
25	20	0.02	4	45	30.18	30.09	22.16
26	30	0.04	6	60	31.10	31.79	22.84
27	40	0.04	2	45	37.65	37.34	27.65
28	30	0.04	4	45	45.57	45.18	33.47
29	30	0.06	4	60	41.65	41.87	30.07

3.3. Physicochemical properties of activated carbons

The SEM images of the ACs are shown in Fig. 1a, 1b, 1c; AC-I and AC-II had much more obvious pores than that of AC-III, and the surfaces of AC-I and AC-II were also rougher than those of AC-III. According to the IUPAC classification [11], the N_2 adsorption/desorption isotherms followed the Type (I) and (IV) curve characteristic of microporous structures, as shown in Fig. 1d, which demonstrates that both micropores and mesopores were exist as the pore structures of the ACs. Table 5 shows that AC-I and AC-II exhibited higher S_{BET}, V_{tot}, S_{mic}/S_{BET} and V_{mic}/V_{tot} than that of AC-III. The results of the Boehm's titration results, element composition and pH_{PZC} values of the ACs are presented in Table 6. AC-III also had a lower content of O, and N as well as basic and acidic groups than the other ACs (AC-I, AC-II), the result conforms to the result of pH_{PZC} value (AC-III>AC-II >AC-I).

In summary, the physicochemical properties of AC-I and AC-II are similar but superior to those of AC-III, because the preparation conditions for AC-I and AC-II are superior to those of AC-III. For example, the excessively high impregnation ratio, activation time and activation temperature were not conducive to the formation of a more developed pore structure inactivated carbon with partial structure loss from combustion. The 3D response surface map in Fig. S3 and the *F* value of the preparation factors indicate that the order of influence of the preparation parameters is the impregnation

Table 4
The adsorption conditions of the ACs

Adsorption conditions	Temperature (°C)	Dose (mg)	pH	C_0 (mg/L)	Q (mg/g)
AC-I	44	0.05	3.5	53	44.57
AC-II	43	0.05	3.5	54	44.56
AC-III	45	0.05	3.5	53	32.69

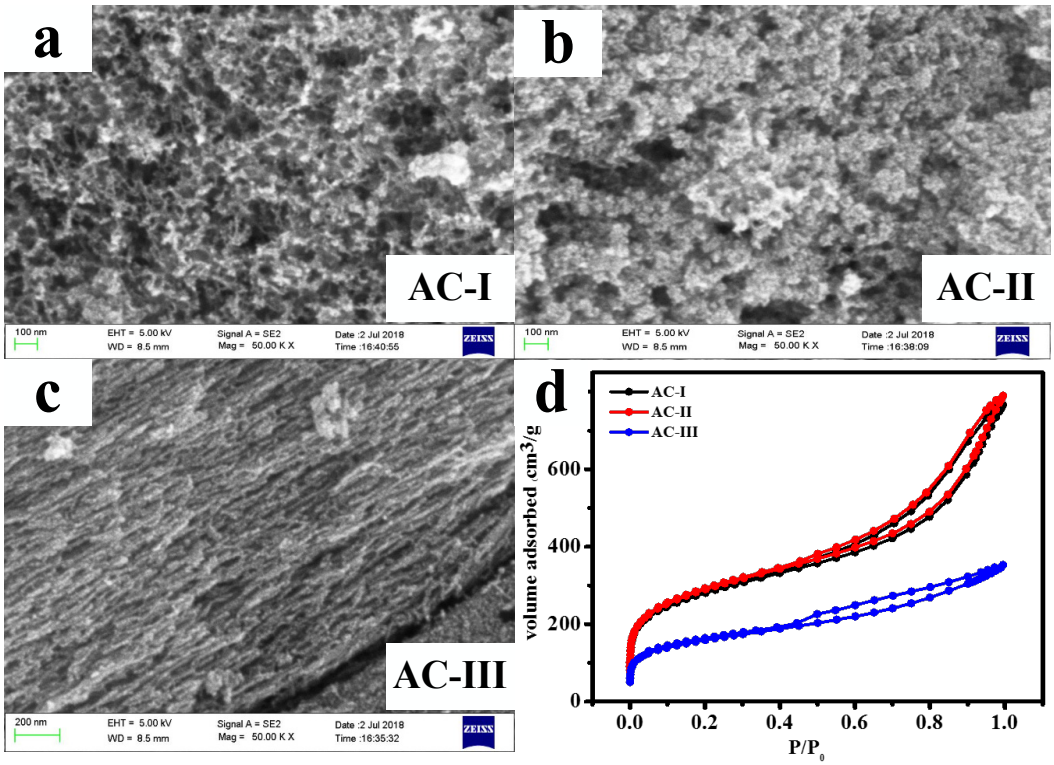

Fig. 1. SEM micrographs of the ACs (a) (b) and (c).N_2 adsorption/desorption isotherms (d).

Table 5

Textural parameters of the ACs

Samples	S_{BET} (m^2/g)	S_{mic} (m^2/g)	S_{mic}/S_{tot} (%)	V_{tot} (cm^3/g)	V_{mic} (cm^3/g)	V_{mic}/V_{tot} (%)	D_p(nm)
AC-I	966.34	429.52	44.45	0.80	0.28	35.22	3.29
AC-II	961.68	418.20	43.49	0.80	0.28	34.69	3.31
AC-III	586.00	148.36	25.32	0.56	0.10	17.18	3.80

Table 6
Boehm's titration results, element composition and pH_{PZC} values of the ACs

Samples	Acidic (mmol/g)	Basic (mmol/g)	Total (mmol/g)	C %	O %	N %	H %	pH_{PZC}
AC-I	2.03	0.18	2.21	56.04	31.51	0.44	5.17	6.05
AC-II	2.01	0.19	2.20	55.78	31.89	0.44	5.67	6.06
AC-III	1.88	0.18	2.06	66.06	22.39	0.38	8.01	6.13

ratio > activation temperature > activation time [28]; they explain that different preparation conditions will obtain activated carbons with different physicochemical properties.

3.4. Adsorption kinetic and adsorption isotherms

As shown in Fig. S4, the pseudo-second-order [29] and Langmuir equation models [30] fit the experimental data quite well, indicating that the adsorption of Cd(II) by activated carbon was both a favorable [31] and chemical adsorption process [32]. Table S4 and Table S5 show that the adsorption capacities of AC-I were greater than those of AC-III, because AC-III had lower microporous proportion and fewer C-/O-functional groups.

3.5. Effects of pH and ionic strength

The initial pH was adjusted with 0.01 M HCl or NaOH to achieve the desired pH value. The solution pH affected not only the number of active sites on the AC-surface, but also

the existing species distribution of cadmium. The Cd(II) ion is the predominant species in an aqueous cadmium chloride solution at pH < 7 [33–35]. Fig. 2a and Fig. 2d show that the removal efficiency was influenced by the solution pH. The removal efficiency of AC-I increased significantly with increasing pH until the removal efficiency or efficiently gradually stabilized when the pH was approximately 6.0. When the organic groups (hydroxy or carboxyl) were released with increasing pH, the hydrogen bond was easily lost, and cation exchange increased the adsorption capacity of Cd(II).The dissociation of acidic functional groups increases the adsorption capacity of Cd(II) by electrostatic attraction [36].

As shown in Fig. 2b, the adsorption capacity of AC-I decreased with increasing ion concentration, because the NaCl competed with Cd(II) ions for the adsorption sites and displaced the Cd(II) to via electrostatic attraction or cation exchange.

3.6. Mechanisms of Cd(II) adsorption

The FTIR result of AC-I is shown in Fig. 3. The most significant peaks of the carbon was in the regions of 3427 cm^{-1} (O-H, carboxyl and phenolgroups), 1627 cm^{-1} (carboxylate), 1384 cm^{-1} (O-H) and 1161 cm^{-1} (C-O) [27,37].

The XPS survey spectra could reveal the different content of carbon and oxygen on the carbons' surfaces. The C1 speaks are shown in Fig. 4, (C-I, C-C/C-H) Sp^2 hybridized graphitized carbon at 284.57 eV; (C-II, C-O) phenolic hydroxyl, alcoholic hydroxyl and ether group at 285.91 eV; (C-III, -COOH) carboxylic groups at 288.18 eV; (C-IV) π-π* transitions at 291.0 eV [38–40]. The major O 1s peak could be fit to 3 curves from the three groups: O-I (carbonyl and quinone, -C=O) at 531.04 eV; O-II (hydroxyl, ether, ester and anhydride groups, C-OH/C-O-C) at 533.08 eV; O-III (carboxylic groups, -COOH) at 535.50 eV [41].

According to the area-simulating curve and calculation of the element area, the contents of each component are shown in Fig. 4. The decrease of the C-II, C-III, O-II and O-III group content of AC-Cd reflected that the lone pair of electrons from O atoms form complexes with Cd(II) (hydroxyl-Cd, carboxyl-Cd complex species). The O-containing functional groups play an important role in the Cd(II) adsorption process according to the following equations [13]:

$$R\text{-}COOH + OH^- \leftrightarrow R\text{-}COO^- + H_2O \quad (7)$$

$$R\text{-}OH + OH^- \leftrightarrow R\text{-}O^- + H_2O \quad (8)$$

$$R\text{-}O^- + Cd(II)X \leftrightarrow R\text{-}O^-M(II)X \quad (9)$$

$$R\text{-}COO^- + Cd(II)X \leftrightarrow R\text{-}COO^-M(II)X \quad (10)$$

where R and Cd(II)X represent special molecules and Cd(II) species, respectively.

In conclusion, adsorption experiments and XPS survey spectra revealed the Cd(II) adsorption mechanism. In addition to the microporous entrapment played a role due to the smaller size of Cd(II) ion. The cation exchange between Cd(II) and hydrogen bond, electrostatic attraction between Cd(II) and oxygen-containing functional group, surface complexation between Cd(II) and O atoms from deprotonated groups (Hydroxyl, carboxyl and other groups).

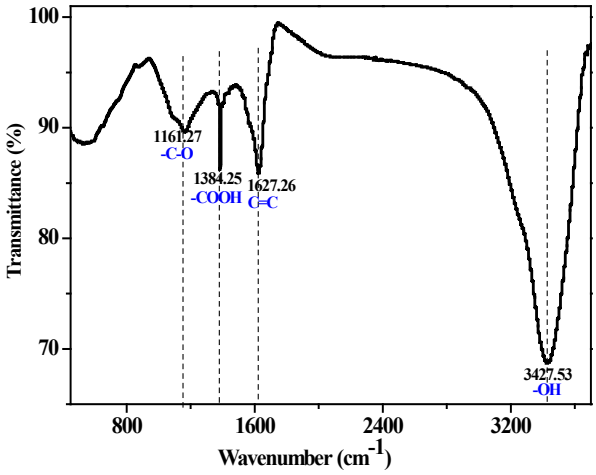

Fig. 3. FTIR spectra of ACs.

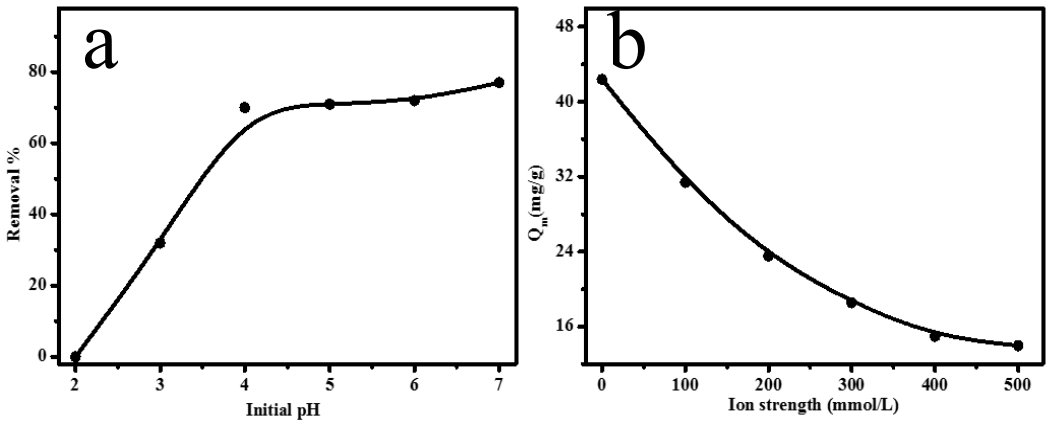

Fig. 2. Effect of initial pH on Cd(II) adsorption, (a) Effect of ionic strengths (NaCl) on Cd(II) adsorption (b).

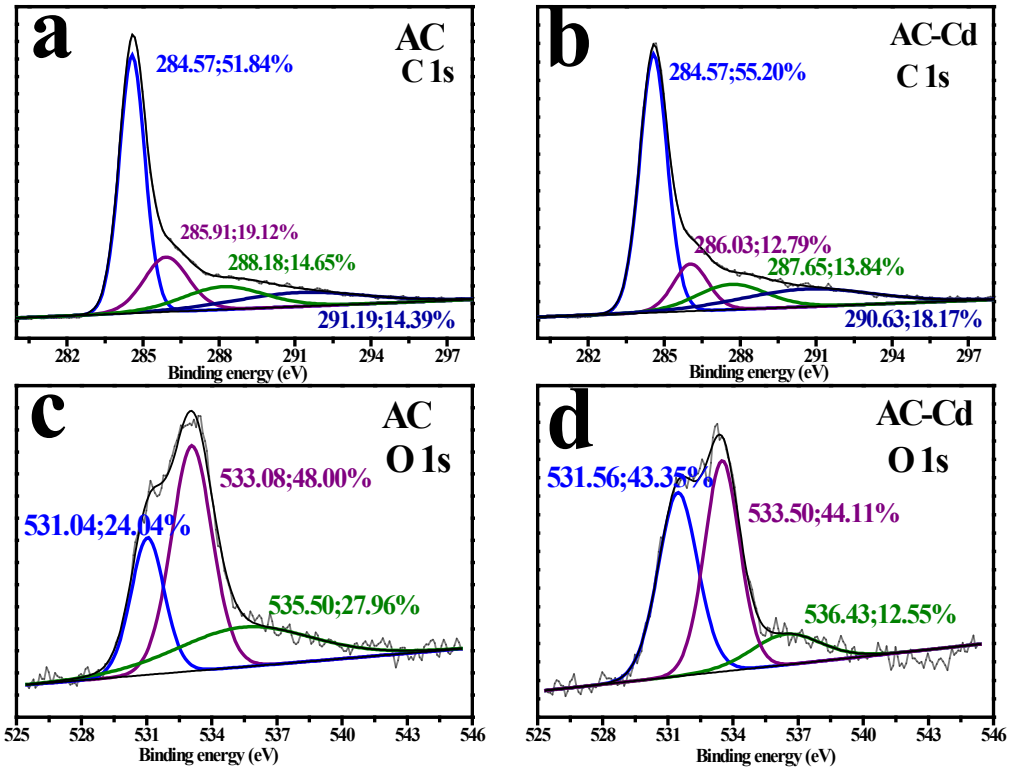

Fig. 4. XPS spectra for carbons before and after Cd (II) adsorption: C 1s (a), (b), and O 1s (c), (d).

Table 7

Comparison of maximum Cd(II) adsorption capacities by various adsorbents

Carbon precursor	Q_{max} (mg/g)	References
Commercial GAC	8.21	[42]
Trapanatans husks	33.80	[43]
Phragmites australis	40.65	[44]
Lotus stalk	39.34	[45]
AC-I	42.85	This work
AC-II	41.44	This work
AC-III	31.02	This work

The comparison of the maximum Cd(II) adsorption capacities (Q_{max}-Cd(II)) of the ACs with other activated carbon derived from other carbon precursors by different modifying methods in Table 7. Generally, AC-III had higher Q_{max}-Cd(II) than other adsorbents, which shown that AC prepared in this experiment could effectively remove Cd(II).

4. Conclusion

In this study, the effects of the preparation and adsorption conditions on the adsorption capacity of Cd(II) were investigated and optimized by response surface methodology (RSM). The preparation conditions of the optimum activated carbon were an impregnation ratio, activation time, activation temperature and adsorption capacity of 2.27, 99.93 min, 510.12°C, and 42.85 mg/g, respectively. The optimized adsorption conditions were: pH, carbon dosage, adsorption temperature, initial concentration and adsorption capacity of 3.51, 0.05 g, 44.57°C, 53.23 mg/L, and 43.55 mg/g. The adsorption mechanism is mainly attributed to microporous entrapment, cation exchange, electrostatic attraction, and surface complexation.

Acknowledgements

This work was supported by National Natural Science Foundation of China (21307078), China Major Science and Technology Program for Water Pollution Control and Treatment (No.2017ZX07101003).

References

[1] E. Dopico, A.R. Linde, E. Garcia-Vazquez, Traditional and modern practices of soil fertilization: Effects on cadmium pollution of river ecosystems in Spain, Hum. Ecol., 37(2) (2009) 235–240.
[2] P.F.A.M. Römkens, H.Y. Guo, C.L. Chu, T.S. Liu, C.F. Chiang, G.F. Koopmans, Prediction of Cadmium uptake by brown rice and derivation of soil-plant transfer models to improve soil protection guidelines, Environ. Pollut., 157(8) (2009) 2435–2444.
[3] F.S. Higashikawa, R.F. Conz, M. Colzato, C.E.P. Cerri, L.R.F. Alleoni, Effects of feedstock type and slow pyrolysis temperature in the production of biochars on the removal of cadmium and nickel from water, J. Clean. Prod., 137 (2016) 965–972.

[4] M.M. Matlock, B.S. Howerton, K.R. Henke, et al. A pyridine-thiol ligand with multiple bonding sites for heavy metal precipitation, J. Hazard. Mater., 82(1) (2001) 55–63.
[5] I.H. Lee, Y.C. Kuan, J.M. Chern, Factorial experimental design for recovering heavy metals from sludge with ion-exchange resin, J. Hazard. Mater., 138(3) (2006) 549–559.
[6] T. Mwamulima, X. Zhang, Y. Wang, S. Song, C. Peng, Novel approach to control adsorbent aggregation: iron fixed bentonite-fly ash for lead (Pb) and cadmium (Cd) removal from aqueous media, Front. Environ. Sci. Eng., 12(2) (2018) 2.
[7] Z. Feng, L. Zhu, Sorption of phenanthrene to biochar modified by base, Front. Environ. Sci. Eng., 12(2) (2018) 1.
[8] J. Su, C. Xie, C. Chen, Y. Yu, G. Kennedy, G.A. Somorjai, P. Yang, Insights into the mechanism of tandem alkene hydroformylation over a nanostructured catalyst with multiple interfaces, J. Am. Chem. Soc., 138(36) (2016) 11568.
[9] Z. Guo, J. Fan, J. Zhang, Y. Kang, H. Liu, L. Jiang, C. Zhang, Sorption heavy metal ions by activated carbons with well-developed microporosity and amino groups derived from Phragmites australis by ammonium phosphates activation, J. Taiwan Inst. Chem. Eng., 58 (2016) 290–296.
[10] Z. Guo, J. Zhang, H. Liu, Y. Kang, Development of a nitrogen-functionalized carbon adsorbent derived from biomass waste by diammonium hydrogen phosphate activation for Cr(VI) removal, Powder Technol., 318 (2017) 459–464.
[11] Z. Guo, X. Bian, J. Zhang, H. Liu, C. Cheng, C. Zhang, J. Wang, Activated carbons with well-developed microporosity prepared from Phragmites australis by potassium silicate activation, J. Taiwan Inst. Chem. Eng., 45(5) (2014) 2801–2804.
[12] Z. Guo, A. Zhang, J. Zhang, H. Liu, Y. Kang, C. Zhang, Anammoniation-activation method to prepare activated carbon with enhanced porosity and functionality, Powder Technol., 309 (2017) 74–78.
[13] Z. Guo, X. Zhang, Y. Kang, J. Zhang, Biomass-derived carbon sorbents for Cd(II) removal: activation and adsorption mechanism, ACS Sustain. Chem. Eng., 5(5) (2017).
[14] H. Liu, P. Dai, J. Zhang, C. Zhang, N. Bao, C. Cheng, L. Ren, Preparation and evaluation of activated carbons from lotus stalk with trimethyl phosphate and tributyl phosphate activation for lead removal, Chem. Eng. J., 228(28) (2013) 425–434.
[15] V. Muthukumar, N. Rajesh, R. Venkatasamy, A. Sureshbabu, N. Senthilkumar, Mathematical modeling for radial overcut on electrical discharge machining of Incoloy 800 by response surface methodology, Procedia Mater. Sci., 6 (2014) 1674–1682.
[16] D. Ozturk, T. Sahan, T. Bayram, A. Erkus, Application of response surface methodology (RSM) to optimize the adsorption conditions of cationic basic yellow 2 onto pumice samples as a new adsorbent, Fresen. Environ. Bull, 26 (2017) 3285–3292.
[17] G. Wang, Y. Wang, Optimization of additives of intumescent fire resistant coating for steel structure by response surface methodology, HuagongXuebao/CIESC J. (2012).
[18] M.A. Bezerra, R.E. Santelli, E.P. Oliveira, L.S. Villar, L.A. Escaleira, Response surface methodology (RSM) as a tool for optimization in analytical chemistry, Talanta, 76(5) (2008) 965–977.
[19] A.H. Basta, V. Fierro, H. El-Saied, A. Celzard, 2-Steps KOH activation of rice straw: An efficient method for preparing high-performance activated carbons, Bioresour. Technol., 100(17) (2009) 3941–3947.
[20] J. Landers, G.Y. Gor, A.V. Neimark, Density functional theory methods for characterization of porous materials, Colloids Surfaces A Physicochem. Eng. Asp., 437(6) (2013) 3–32.
[21] H.P. Boehm, Chemical Identification of Surface Groups, Adv. Catal., 16 (1996) 179–274.
[22] T. Chmiel, M. Kupska, W. Wardencki, J. Namieśnik, Application of response surface methodology to optimize solid-phase microextraction procedure for chromatographic determination of aroma-active monoterpenes in berries, Food Chem., 221 (2017) 1041–1056.
[23] Y. Liu, F. Liu, L. Ni, M. Meng, X. Meng, G. Zhong, J. Qiu, A modeling study by response surface methodology (RSM) on Sr(ii) ion dynamic adsorption optimization using a novel magnetic ion imprinted polymer, RSC Adv., 6(60) (2016) 54679–54692.
[24] F. Nasiri Azad, M. Ghaedi, K. Dashtian, A. Jamshidi, G. Hassani, M. Montazerozohori, S. Hajati, M. Rajabi, A.A. Bazrafshan, Preparation and characterization of an AC-Fe_3O_4-Au hybrid for the simultaneous removal of Cd^{2+}, Pb^{2+}, Cr^{3+} and Ni^{2+} ions from aqueous solution via complexation with 2-((2,4-dichloro-benzylidene)-amino)-benzenethiol: Taguchi optimization, RSC Adv., 6(24) (2016) 19780–19791.
[25] A. Witek-Krowiak, K. Chojnacka, D. Podstawczyk, A. Dawiec, K. Pokomeda, Application of response surface methodology and artificial neural network methods in modelling and optimization of biosorption process, Bioresour. Technol., 160(5) (2014) 150–160.
[26] L. Lu, Z. Yang, P. Sun, J. Huang, Optimization of the biosorption of Pb^{2+} by citron peel using response surface methodology, Acta Scientiae Circumstantiae (2009).
[27] M. Dastkhoon, M. Ghaedi, A. Asfaram, A. Goudarzi, S.M. Mohammadi, S. Wang, Improved adsorption performance of nanostructured composite by ultrasonic wave: Optimization through response surface methodology, isotherm and kinetic studies, Ultrason. Sonochem., 37 (2016) 94.
[28] B. Kiran, A. Kaushik, C.P. Kaushik, Response surface methodological approach for optimizing removal of Cr (VI) from aqueous solution using immobilized cyanobacterium, Chem. Eng. J., 126(2) (2007) 147–153.
[29] M.K. Aroua, S.P.P. Leong, L.Y. Teo, C.Y. Yin, W.M.A.W. Daud, Real-time determination of kinetics of adsorption of lead(II) onto palm shell-based activated carbon using ion selective electrode, Bioresour. Technol., 99(13) (2008) 5786–5792.
[30] I. Langmuir, The adsorption of gases on plane surfaces of glass, mica and platinum, J. Am. Chem. Soc. (1918).
[31] G. Crini, H.N. Peindy, F. Gimbert, C. Robert, Removal of C.I. Basic Green 4 (Malachite Green) from aqueous solutions by adsorption using cyclodextrin-based adsorbent: Kinetic and equilibrium studies, Sep. Purif. Technol., 53(1) (2007) 97–110.
[32] P. Chingombe, B. Saha, R.J. Wakeman, Sorption of atrazine on conventional and surface modified activated carbons, J. Colloid Interface Sci., 302(2) (2006) 408–416.
[33] H. Liu, Q. Gao, P. Dai, J. Zhang, C. Zhang, N. Bao, Preparation and characterization of activated carbon from lotus stalk with guanidine phosphate activation: Sorption of Cd(II), J. Anal. Appl. Pyrolysis, 102(102) (2013) 7–15.
[34] H. Liu, S. Liang, J. Gao, H.H. Ngo, W. Guo, Z. Guo, Y. Li, Development of biochars from pyrolysis of lotus stalks for Ni(II) sorption: Using zinc borate as flame retardant, J. Anal. Appl. Pyrolysis, 107(9) (2014) 336–341.
[35] Z. Guo, J. Zhang, H. Liu, Y. Kang, J. Yu, C. Zhang, Optimization of the green and low-cost ammoniation-activation method to produce biomass-based activated carbon for Ni(II) removal from aqueous solutions, J. Clean. Prod., 159 (2017) 38–46.
[36] P. Yuan, M. Fan, D. Yang, H. He, D. Liu, A. Yuan, J.X. Zhu, T.H. Chen, Montmorillonite-supported magnetite nanoparticles for the removal of hexavalent chromium [Cr(VI)] from aqueous solutions, J. Hazard. Mater., 166 (2009) 821–829.
[37] Z. Ma, H. Ming, H. Huang, Y. Liu, Z. Kang, One-step ultrasonic synthesis of fluorescent N-doped carbon dots from glucose and their visible-light sensitive photocatalytic ability, New J. Chem., 36(4) (2012) 861–864.
[38] J.L. Figueiredo, M.F.R. Pereira, The role of surface chemistry in catalysis with carbons, Catal. Today, 150 (2010) 2–7.
[39] S. Yang, T. Xiao, J. Zhang, Y. Chen, L. Li, Activated carbon fiber as heterogeneous catalyst of peroxymonosulfate activation for efficient degradation of Acid Orange 7 in aqueous solution, Sep. Purif. Technol., 143 (2015) 19–26.
[40] S. Biniak, G. Szymański, J. Siedlewski, A. Światkoski, The characterization of activated carbons with oxygen and nitrogen surface groups, Carbon, 35 (1997) 1799–1810.
[41] K.J.H. and W.P.H. U. ZIELKE, U. Zielke, K.J. Hüttinger, W.P. Hoffman, Surface-oxidized carbon fibers: I. Surface structure and chemistry, Carbon, 34 (1996) 983–998.

[42] M.J. Puchana-Rosero, M.A. Adebayo, E.C. Lima, F.M. Machado, P.S. Thue, J.C.P. Vaghetti, C.S. Umpierres, M. Gutterres, Microwave-assisted activated carbon obtained from the sludge of tannery-treatment effluent plant for removal of leather dyes, Colloids Surfaces A Physicochem. Eng. Asp., 504 (2016) 105–115.
[43] W. Yin, C. Zhao, J. Xu, J. Zhang, Z. Guo, Y. Shao, Removal of Cd(II) and Ni(II) from aqueous solutions using activated carbon developed from powder-hydrolyzed-feathers and Trapanatans husks, Colloids Surfaces A Physicochem. Eng. Asp., 560 (2019) 426–433.
[44] Z. Guo, X. Zhang, Y. Kang, J. Zhang, Biomass-derived carbon sorbents for Cd(II) removal: Activation and adsorption mechanism, ACS Sustain. Chem. Eng., 5(5) (2017) 4103–4109.
[45] H. Liu, P. Dai, J. Zhang, C. Zhang, N. Bao, C. Cheng, L. Ren, Preparation and evaluation of activated carbons from lotus stalk with trimethyl phosphate and tributyl phosphate activation for lead removal, Chem. Eng. J., 5(5) (2017) 4103–4109.

Supplementary material

Calculation of parameters for adsorbent pores

Pore size distribution was determined by the Density Functional Theory (DFT) method. Micropore volume (V_{mic}), micropore surface area (S_{mic}) and external surface area (S_{ext}) were calculated using the t-plot method. The total pore volume (V_{BJH}) was deduced from the manufacturer's software by the BJH theory.

FTIR

The FTIR spectra of the carbons were recorded from 400 to 4000 cm^{-1} by using a Fourier transform infrared spectrometer (Fourier-380FT-IR, USA).

XPS

XPS was used to qualitatively and quantitatively determine the element and functional groups on/near the carbons' surfaces. All binding energies were referenced to the C 1s peak at 284.6 eV to correct the surface charging effects.

Boehm titration method

Boehm titration method is a commonly used method for determination of surface acid oxygen containing functional groups the principle of the method is based on different intensity of alkali and different oxygen containing functional groups on the surface of the reaction for qualitative and quantitative analysis, according to the literature research think sodium bicarbonate and carboxyl sodium carbonate and carboxyl and lactone, sodium hydroxide and carboxyl lactone and phenol hydroxyl, ethanol and sodium carboxyl lactone base phenolic hydroxyl and carbonyl so the corresponding content of oxygen containing functional groups can be calculated according to the quantity of consumption of alkali specific operation is as follows: preparation of 0.1 N respectively ethanol sodium sodium hydroxide, sodium carbonate. Sodium bicarbonate and hydrochloric acid standard solution, take 25 ml to 100 ml of plug taper bottle, add 0.5 g of water chestnut skin biochar respectively. Then put the conical flask on the thermostatic oscillator oscillating at room temperature for 24 h, filtering, and deionized water will be on the surface of the filter paper and biochar free alkali into the filtrate With calibration titration of hydrochloric acid solution, finally to the introduced four kinds of alkali consumption of standard solution, calculate the corresponding content of oxygen containing functional groups

Isoelectric point (PZC)

Preparation of 50 ml, NaCl solution of 0.01 N in 8 100 ml conical flask With sodium bicarbonate and hydrochloric acid to pH 2 to 12 and then add 0.15 g of water chestnut

Table S2
Results of regression analysis of model-I

Source	Sum of squares (SS)	Df	Mean squares (MS)	*F*	*P*
Model	2206.43	9	245.16	197.54	< 0.0001
A	287.89	1	287.89	231.97	< 0.0001
B	150.81	1	150.81	121.52	< 0.0001
C	67.34	1	67.34	54.26	0.0002
AB	95.68	1	95.68	77.09	< 0.0001
AC	100.3	1	100.3	80.82	< 0.0001
BC	18.23	1	18.23	14.69	0.0064
A^2	896.86	1	896.86	722.64	< 0.0001
B^2	347.97	1	347.97	280.37	< 0.0001
C^2	64.67	1	64.67	52.11	0.0002
Residual	8.69	7	1.24		
Lack of Fit	2.59	3	0.86	0.57	0.6663

Table S1
Equation of models

Model	Equation	
Model-I	$Y = -300.60316 + 72.41130 \times A + 2.12866 \times B + 0.60719 + 0.22144 \times A \times B - 0.050$	(3)
	$75A \times C - 7.11667 \times 10^{-4} \times B \times C - 15.18987 \times A^2 - 0.011351 \times B^2 - 4.13982 \times 10^{-4} \times C^2$	
Model-II	$Y = +45.60 + 3.05 \times A + 8.28 \times B - 2.60 \times C + 5.21 \times D - 0.88 \times A \times B + 0.15 \times A \times C + 1.0$	(4)
	$8 \times A \times D - 2.87 \times B \times C + 1.64 \times B \times D - 1.23 \times C \times D - 4.61 \times A^2 - 11.45 \times B^2 - 8.77 \times C^2 - 7.30 \times D^2$	
Model-III	$Y = -172.92520 + 2.89859 \times A + 2811.22825 \times B + 19.96614 \times C + 2.6787 \times D - 1.8$	(5)
	$0999 \times A \times B + 9.21781 \times 10 - 3 \times A \times D - 66.93914 \times B \times C + 5.90666 \times B \times D - 0.03$	
	$2451 \times C \times D - 0.049007 \times A^2 - 2.14817 \times C^2 - 0.030017 \times D^2$	
Model-IV	$Y = -129.59371 + 1.88516 \times A + 2287.50924 \times B + 14.23458 \times C + 2.08689 \times D - 3.$	(6)
	$62069 \times A \times B + 2.625 \times 10 - 3 \times A \times C + 6.13333 \times 10 - 3 \times A \times D - 1.02586 \times B \times C$	
	$+3.30345 \times B \times D - 0.030167 \times C \times D - 0.030205 \times A^2 - 1.76856 \times C^2 - 0.022513 \times D^2$	

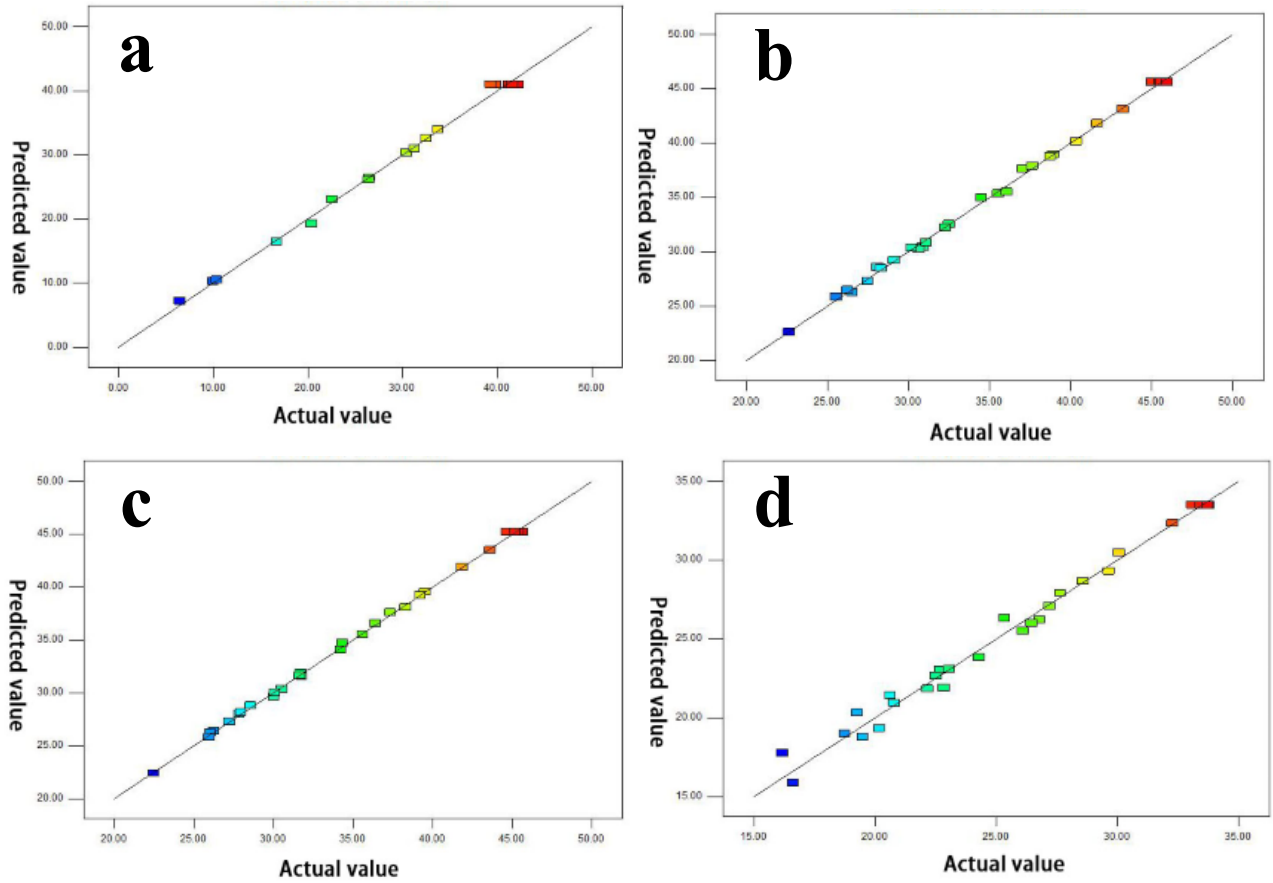

Fig. S1. The linear plot between the predicted values of the model and the experimental values under the corresponding conditions.

Table S3
Results of regression analysis of model II, III, IV

Source	Model-II					Model-III					Model-IV				
	SS	*Df*	*MS*	*F*	*P*	*SS*	*Df*	*MS*	*F*	*P*	*SS*	*Df*	*MS*	*F*	*P*
Model	1406.78	14	100.48	518.66	< 0.0001	1393.94	14	99.57	772.24	< 0.0001	816.46	14	58.32	77.72	< 0.0001
D	107.67	1	107.67	555.73	< 0.0001	107.18	1	107.18	831.32	< 0.0001	53.39	1	53.39	71.15	< 0.0001
E	177.57	1	177.57	916.55	< 0.0001	175.29	1	175.29	1359.53	< 0.0001	131.59	1	131.59	175.36	< 0.0001
F	78.55	1	78.55	405.46	< 0.0001	82.29	1	82.29	638.21	< 0.0001	70.62	1	70.62	94.11	< 0.0001
G	314.78	1	314.78	1624.74	< 0.0001	338.64	1	338.64	2626.48	< 0.0001	171.26	1	171.26	228.23	< 0.0001
DE	1.86	1	1.86	9.58	0.0079	0.32	1	0.32	2.46	0.1394	1.27	1	1.27	1.69	0.2148
DF	0.087	1	0.087	0.45	0.5133	1.14E-03	1	1.14E-03	8.87E-03	0.9263	1.10E-02	1	1.10E-02	0.015	0.9052
DG	4.66	1	4.66	24.04	0.0002	7.65	1	7.65	59.31	< 0.0001	3.39	1	3.39	4.51	0.052
EF	19.89	1	19.89	102.67	< 0.0001	17.33	1	17.33	134.38	< 0.0001	4.07E-03	1	4.07E-03	5.42E-03	0.9423
EG	6.51	1	6.51	33.61	< 0.0001	7.59	1	7.59	58.85	< 0.0001	2.37	1	2.37	3.16	0.097
FG	6.06	1	6.06	31.28	< 0.0001	3.79	1	3.79	29.4	< 0.0001	3.28	1	3.28	4.37	0.0554
D^2	138.12	1	138.12	712.89	< 0.0001	155.78	1	155.78	1208.24	< 0.0001	59.18	1	59.18	78.86	< 0.0001
E^2	200.46	1	200.46	1034.69	< 0.0001	210.1	1	210.1	1629.53	< 0.0001	148.01	1	148.01	197.24	< 0.0001
F^2	499.11	1	499.11	2576.17	< 0.0001	478.92	1	478.92	3714.48	< 0.0001	324.62	1	324.62	432.6	< 0.0001
G^2	345.63	1	345.63	1783.99	< 0.0001	295.88	1	295.88	2294.83	< 0.0001	166.44	1	166.44	221.8	< 0.0001
Residual	2.71	14	0.19			1.81	14	0.13			10.51	14	0.75		
Lack of Fit	2.18	10	0.22	1.63	0.3373	1.26	10	0.13	0.94	0.5788	10.22	10	1.02	14.16	0.0105

skin biochar respectively, put the conical flask on the thermostatic oscillator oscillating 2 h at room temperature, let stand for 24 h, the solution of the pH is measured by pH meter in the abscissa denotes the original pH, the reaction

Table S4
Parameters of kinetics models and intra-particle diffusion model for the sorption of Cd(II) onto the carbons

Kinetic models	parameters	AC-III	AC-I
Pseudo-first-order	K_1 (1/min)	0.1475	0.9641
	Q_{cal} (mg/g)	12.04	26.58
	R^2	0.9413	0.9622
Pseudo-second-order	K_2 (g/(mg min))	0.1396	0.1422
	Q_{cal} (mg/g)	20.29	26.25
	R^2	0.9963	0.9976

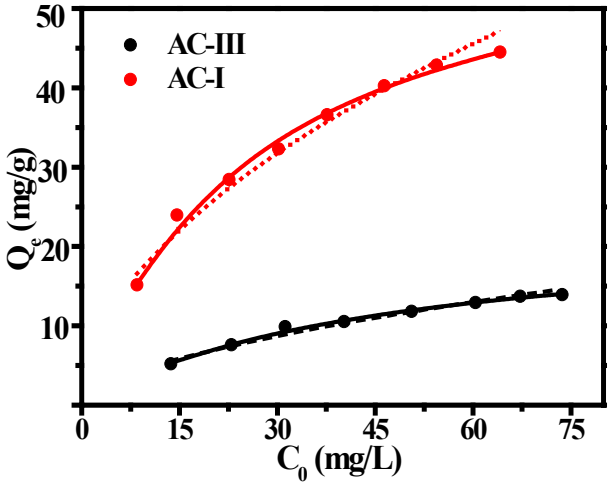

Fig. S3. Adsorption isotherms of carbons fitted by Langmuir model (solid lines) and Freundlich model (dash lines).

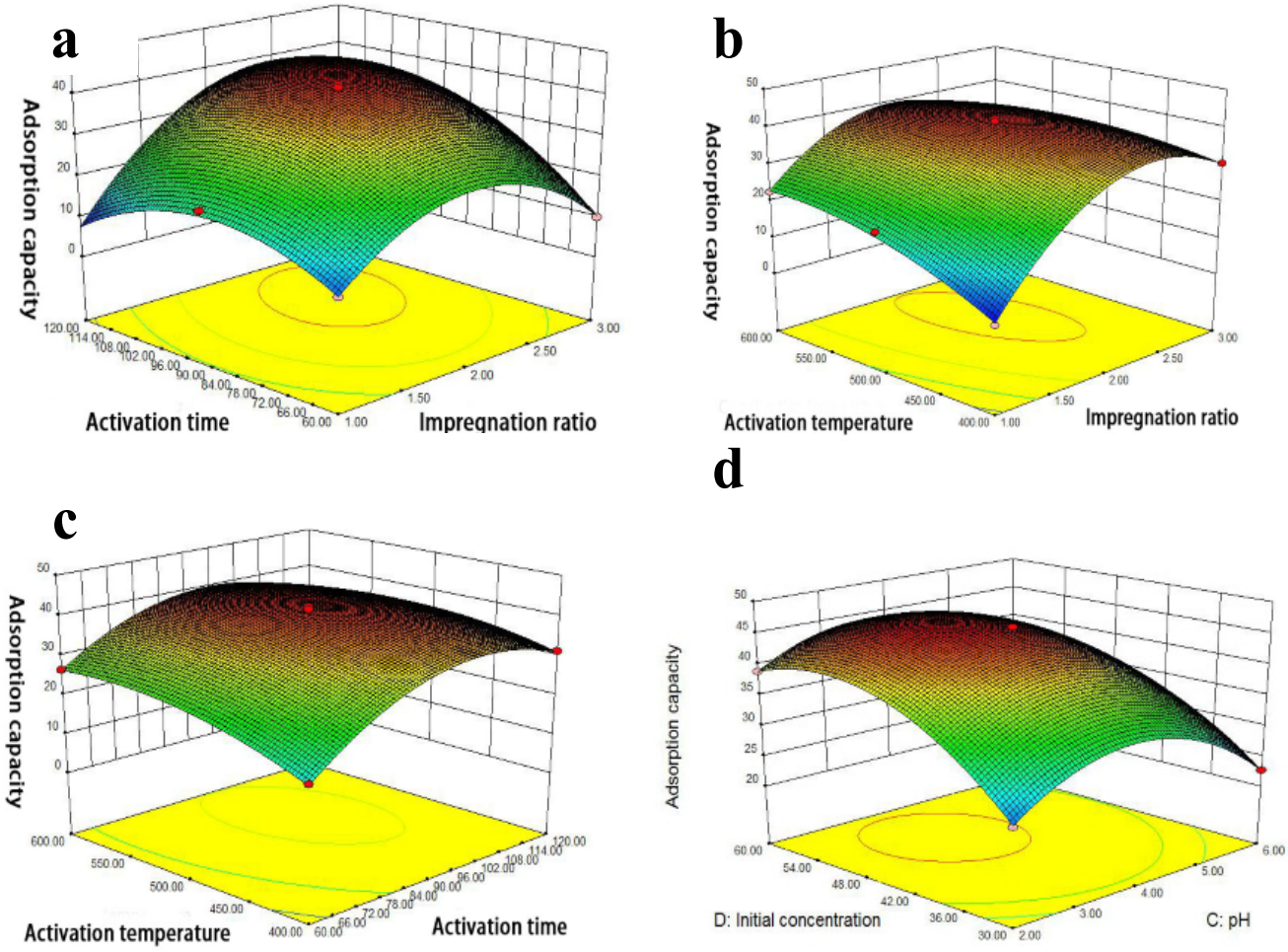

Fig. S2. Effect of preparation conditions on adsorption capacity: (a) impregnation ratio and activation time; (b) impregnation ratio and activation temperature; (c) activation time and activation temperature.

Table S5
Langmuir and Freundlich isotherm constants for Cd(II) adsorption onto carbons

Model	parameters	AC-III	AC-I
Langmuir	Q_m (mg/g)	17.828	50.437
	K_L (L/mg)	23.8	38.3
	R^2	0.9924	0.9948
Freundlich	K_F ((mg/g)/(L/mg)$^{1/n}$)	1.006	4.288
	1/n	0.5718	0.528
	R^2	0.9915	0.9836

after pH as ordinate plot After the initial pH and reaction pH as the abscissa value equal to the corresponding water chestnut skin biochar isoelectric point.

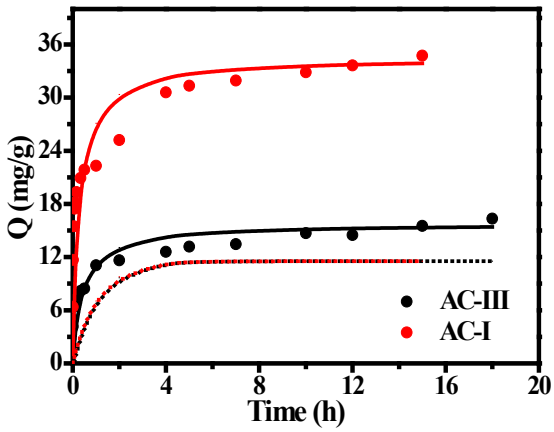

Fig. S4. Adsorption kinetics fitted by pseudo-first order (solid lines) and pseudo-second-order models (solid lines).